



Thorax x-ray image segmentation technique using four variants of thresholding algorithm

Rio Subandi^{*1}, Herman², Anton Yudhana¹

Master Program of Informatics, Universitas Ahmad Dahlan, Yogyakarta, Indonesia¹

Department of Electrical Engineering, Universitas Ahmad Dahlan, Yogyakarta, Indonesia²

Article Info

Keywords:

Pneumonia, Segmentation, Thresholding

Article history:

Received: July 31, 2023

Accepted: December 05, 2023

Published: February 28, 2024

Cite:

R. Subandi, Herman, and A. Yudhana, "Thorax X-Ray Image Segmentation Technique Using Four Thresholding Algorithm Variants", KINETIK, vol. 9, no. 1, Feb. 2024.

Retrieved from

<https://kinetik.umm.ac.id/index.php/kinetik/article/view/1809>

*Corresponding author.

Rio Subandi

E-mail address:

riosubandi9@gmail.com

Abstract

Pneumonia is a respiratory infection caused by bacteria, viruses or fungi, and has been recognized as a fairly common and threatening disease. When diagnosing this disease, doctors usually also use thorax X-ray images. Nowadays, diagnosing pneumonia has been made possible with the help of machine learning technology. Doctors or medical personnel in locations where there are no pulmonary specialists or experts can be assisted by this technology. Machine learning algorithms are used to process digital images that have passed the pre-processing and segmentation stages. This paper offers a solution to segmentation technique of thorax X-ray digital image using a combination of four thresholding algorithms. This combination aims to find the best CNN model with segmentation techniques in the form of the most suitable thresholding algorithm. The result of this research is four different data sets. The thresholding algorithms used include binary, thresh binary inv, thresh to zero, thresh to zero inv with a threshold value of 150. The data used in this research is a thorax X-ray image dataset, as many as 5,856 images acquired from the Kaggle repository data. The program code in this research uses the Python programming language in the Anaconda environment. This research has resulted in a comparison of the accuracy values obtained using 4 variants between thres_binary thresholding algorithm and thres_binary_inv. The thres_tozero obtained 95% of accuracy while thres_tozero_inv obtained 94% of accuracy.

1. Introduction

Pneumonia is a common disease in the chest area that affects many people [1][2][3][4]. In clinical practice, radiologists have to review multimodal information to screen pneumonia cases from tremendous clinical data. Oftentimes, this task relies on manual operations by experts, which is time-consuming and prevents fully automated assessment. Therefore, it is necessary and important to develop a fast, robust, and accurate Computer Aided Diagnosis (CAD) system to perform an automated pneumonia screening [5]. Pneumonia is a respiratory infection caused by bacteria, viruses or fungi, and has been recognized as a fairly common and life-threatening disease for the past two centuries. The prevalence of pneumonia is quite high in extreme age groups [6]. Approximately 450 million people (about 7% of the world's population) are diagnosed with pneumonia each year, and about 4 million deaths have been reported [7].

In the era of evolving medical technology, thorax X-ray image diagnosis plays an important role in monitoring and diagnosing pneumonia. One of the main steps in thorax X-ray image analysis is segmentation, which aims to separate important structures such as lungs and other structures from the image background. Improved thorax X-ray image segmentation techniques are highly relevant considering their important role in the screening and diagnosis of pneumonia. In this study, the latest and most effective thorax X-ray image segmentation technique using four different threshold algorithms will be described.

Artificial intelligence is intelligence added to systems that can be managed in a scientific context, or it can also be called intelligence in scientific units. This type of artificial intelligence is based on the principle that human intelligence can be defined in such a way that machines can also imitate and perform tasks from the simplest to the more complex. The purpose of artificial intelligence is to perform learning, reasoning and perception [8]. One of the image processing techniques is machine learning. Machine learning is a computational method that combines statistics and computer science to produce algorithms that can recognize input data [9]. In addition to machine learning, there are other image processing techniques, namely deep learning, which is better than machine learning [10].

This research has high urgency in the medical field. In practice, thorax X-ray image segmentation technology can help doctors diagnose lung diseases such as pneumonia, lung cancer, and tuberculosis. Through accurate segmentation results, doctors can more precisely determine the area affected by the disease, making treatment more effective and efficient. In addition, chest X-ray image segmentation technology can also help medical research, such as the development of computer systems to automatically diagnose lung diseases. In this research, thorax X-ray image segmentation technology forms an important component of the developed system. Therefore, this research is urgent for improving the quality of healthcare and developing medical technology.

The use of threshold algorithms in thorax X-ray image segmentation has become an increasingly important research topic. However, there are many challenges to overcome, including differences in figure contrast, the presence of shadows, and anatomical differences between patients. Therefore, an in-depth understanding of the proper use of threshold algorithms is essential to obtain accurate segmentation results.

One way to tell if a patient has pneumonia is by looking at raw images or CT scans of the patient's lungs. Until now, medical personnel have analyzed directly by examining the results of the patient's lung samples without using a computer [11]. This study aims to recommend four variants of threshold algorithms adapted to improve the accuracy of thorax X-ray image segmentation. Each algorithm is tested and evaluated to understand its performance in overcoming the challenges of thorax X-ray images. The main objective of this research is to provide a deeper understanding of the use of threshold algorithms and introduce innovations in the field of thorax X-ray image segmentation, which is expected to make a positive contribution to the diagnosis of lung-pneumonia diseases. In this study, the Pneumonia Segmentation method was applied. Based on the description above, the purpose of the study was to obtain results based on 4 thresholding variation methods using thresh binary, thresh binary inv, thresh to zero, and thresh to zero inv with three threshold values 150.

Based on some previous researches related to this research as follows [12], various threshold-based techniques are used in the theory of vegetation image segmentation to identify similarities between vegetation and other partially visible objects in the image. The first segmentation technique is input image, and then image preprocessing. After preprocessing, semantic segmentation is carried out using thresholding such as the first step threshold setting, the second step features extraction, and the third step classification. Furthermore, the segmentation results. The results of the sophisticated transformation of semantic segmentation techniques to accommodate different data patterns and features of agricultural images.

The thorough analysis of these networks covers everything from the different techniques employed by deep learning methods to a quick synopsis of more conventional techniques (graphical models and forest-based machine learning techniques). Markov random fields (MRFs) and their variant conditional random fields were the graphical methods that were first used for labeling large-scale urban networks. The majority of these techniques use region growth algorithms to segment data into homogeneous superfacets in three steps. The RF-MRF framework is used for the classification and refinement of the superfacets into the proper classes. Modeling the segmentation of elements into homogeneous segments such as super facets typically uses unsupervised clustering-based algorithms such as region growth methods in Urban-LODs, variational shape approximation (VSA) for extracting planar structures in VBM, and orthogonal grids sampled from 2D image projections of the input mesh in USM. The machine learning method uses the ... The predicted label probabilities are refined using the MRF (energy minimization) framework, which improves the spatial coherence between superfacets and the context clarity across class boundaries. For mesh surface labeling, superfacet-based classification with randomized decision trees was also utilized in the creation of the SUM benchmark dataset of urban-scale meshes. End-to-end trained deep learning methods, e.g. learning facial features of 3D meshes were used for face-based classification (face-based semantic segmentation), and classifying these methods into appropriate categories with a detailed description of how they achieve mesh classification of urban elements [13].

By utilizing the ensemble method, three different types of X-ray images were classified. Each image is first processed through a classification layer to determine if it is COVID-19, pneumonia, or normal image. To segment the affected region of the X-ray image, train and test a U-Net segmentation model based on DenseNet103 architecture as a backend once the ground truth dataset is ready. The input X-ray image is classified by the ensemble classification model, and the segmentation model groups the impacted area as a predicted mask of the input image. The final predicted segmentation image is then obtained by superimposing the predicted mask on the input image. Grad-CAM has been used to identify the image regions that positively contribute to the COVID-19 and pneumonia classes. The Amazon SageMaker Ground Truth Tool was then used to crop the highlighted portion in order to produce a ground truth mask, which was subsequently used to train the U-Net segmentation model. This model is a modified version of the DenseNet103 frame encoder (downsampler) and decoder (upsampler) model, which is a U-Net. It predicts an output mask using an input image and a ground truth masks [14].

Another study conducted a comprehensive survey on proper boundary recovery for semantic segmentation, focusing mainly on 2D images and 3D point clouds. They formulated a potential boundary recovery problem for semantic segmentation based on DCNN, outlining the terminology as well as background concepts in this field. They categorized the boundary recovery methods into four strategies according to their techniques and network architectures to discuss

how they obtain accurate semantic segmentation boundaries. Furthermore, publicly available datasets where they have been assessed are debated [15].

Deep learning and other JSTs are inspired by biological neural networks and mathematically construct a network model with multiple connected layers. The first network layer (called the input layer) receives input (e.g. a slide image). It has a set of parameters and can be used to calculate the output. Thus, each successive network layer receives input from the previous layer, uses its parameters, and calculates an output. In the end, the last network layer (called the output layer) calculates the output of the entire model. Because they do not directly produce or receive model outputs, the layers that sit between the input and output layers are known as hidden layers because they are invisible. CNNs have not only been used for image classification but also for pathology image segmentation. To segment an image for large data (like a whole slide pathology image), the image is first split up into numerous small patches. These patches are classified by CNNs through training, and patches belonging to the same class are aggregated into a single segmented region. The use of tiny patches can result in fine spatial segmentation resolution. However, the patches need to be large enough to be classified accurately using matlab tools [16]. The similarities from the previous studies are both used segmentation methods and pneumonia objects. The difference is in the methods and results.

2. Research Method

This research consists of several stages, starting from the acquisition of data to be used in the research, preprocessing, segmentation, classification process and evaluation of classification results.

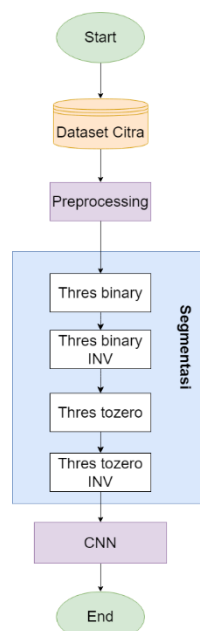


Figure 1. Research Stages

Figure 1 explains the stages of the research, namely dataset input and preprocessing. The preprocessing stage included resizing and image conversion. The next stage of the segmentation was used to separate the background objects in the image by using 4 thresholding types, namely `thresh_binary`, `thresh_binary_inv`, `thresh_tozero` and `thresh_tozero_inv`. Then, the results of the segmentation were carried out by the CNN algorithm.

2.1 Dataset

The pneumonia dataset used was retrieved from Kaggle data repository, consisting of the Chest X-Ray Images of patients who might have pneumonia. This dataset was created by Dr. Paul Mooney which was published on January 1, 2019 with a jpeg figure format. The total number of data published was 5,856 and the copyright of this dataset was under the CC BY-NC-SA 4.0 license. This dataset consisted of two classes, i.e. pneumonia and normal. This dataset was used for non-commercial purposes. This metadata makes it easy to help users understand the processing of pneumonia dataset from (www.kaggle.com).

2.2 Preprocessing

Preprocessing was the initial stage in image processing that aimed to clean, prepare, and transform raw images into a form that was easier and more relevant for further processing [17]. The preprocessing stage included cropping

the figure at certain coordinates and scale [18]. The first preprocessing stage of the dataset was normalized, the output of normalization was then resized and converted RGB image into grayscale.

2.3 Segmentation

Segmentation is dividing an image into regions or objects within it [19]. Segmentation was the first step in performing digital image feature extraction. This process isolated image elements with the same characteristics. There were several stages in the segmentation process, starting from converting RGB images into grayscale images, converting grayscale images into binary images, complement operations, and morphological operations [20]. The segmentation process has been used in various applications and digital image processing, such as fingerprint authentication, imaging in the field of medicine, satellite images, and others [21].

The general steps to perform image segmentation started by analyzing the image and determining the number of regions required for segmentation. Secondly, selecting a segmentation technique by using thresholding. Third, determining the number of thresholds required for image segmentation. Fourth, applying thresholding techniques to the image to get the optimal threshold. Fifth, the result of image threshold segmentation was divided into several regions to separate the object and background.

Segmentation in this study used thresholding techniques. Thresholding technique aimed to convert the intensity of pixels in the image into binary values based on a certain threshold value [22]. If the pixel value is greater than the threshold value, a white value is given, while a smaller pixel value is given a black value. Segmentation was also used to divide the image into constituent parts that have important information [23]. This segmentation used 4 thresholding techniques `thresh_binary`, `thresh_binary_inv`, `thresh_tozero`, and `thresh_tozero_inv`.

The `thresh_binary` method converted pixels into two values only, i.e. 0 or 1. If the pixel intensity exceeds a certain threshold, it will be converted to 1, otherwise, it will be converted to black. `Thresh_binary_inv` was similar to the previous method, but the color change was reversed. Pixels that exceed the threshold will be converted to 0 and vice versa. `Thresh_tozero` in this method, pixels with intensity lower than the threshold will be converted to zero (black). Meanwhile, pixels with an intensity higher than the threshold do not undergo `Thresh-tozero_inv` changes: Same as the `Thresh_tozero` method but the opposite of the result. Pixels with intensity lower than the threshold will remain while pixels with an intensity higher than that will be converted to zero (black) [24].

2.4 CNN

Image classification can be done using the CNN method, which is capable of automatically extracting hierarchical features from images. Convolutional Neural Network (CNN) method also known as ConvNet or CNN is a deep learning technique consisting of many layers. CNN is a development of the conventional ANN (Artificial Neural Network). CNN processes the image through a network of layers and produces an output of a certain class. Each layer performs learning. The output of each layer is used as input for the next layer. At the beginning of the network, the layer produces simple features such as color, brightness and edges. Subsequently, it will produce more complex features [25].

Convolutional Neural Network (CNN) is a type of deep learning designed to process two-dimensional data into higher networks (Sriyati et al., 2020). CNN uses convolutional operations that apply filters in each input section first to extract patterns and this makes CNN unique compared to other artificial neural networks. CNN uses a Graphics Processing Unit (GPU) for the computational process, in other words, when using the Nvidia Cuda platform, processing can be much faster than using a Central Processing Unit (CPU) [26]. The CNN architecture can be seen in Figure 2.

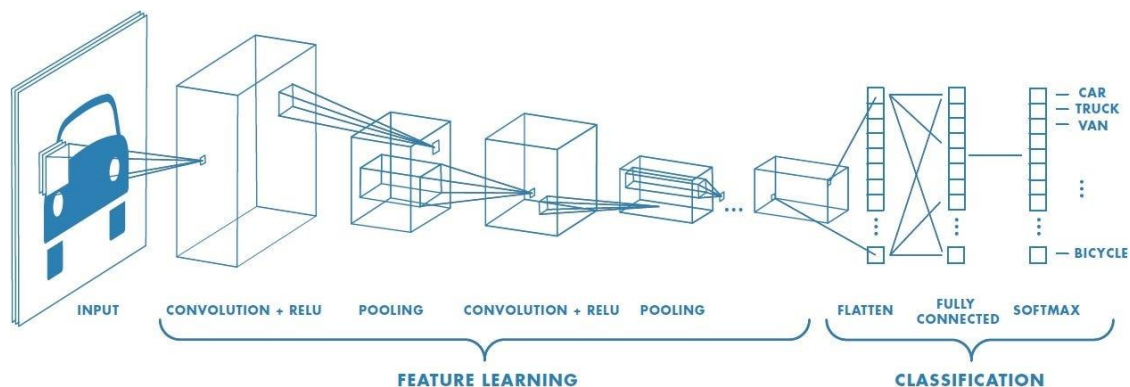


Figure 2 Process of Convolution Neural Network

Figure 2 is the process of CNN, it can be seen from the figure that the process is divided into 2 stages, namely feature learning and classification. Feature learning consists of an input layer which is then abstracted into a feature

map value, a two-dimensional convolution layer. The output of the convolutional layer in the form of a kernel will be pooled to minimize or reduce the layer. The pooling result will become a new input layer that will be processed the same as before.

2.5 Evaluation Model

The model testing stage is the most important stage in this research because this stage is carried out to test the algorithm used. The proposed model then considered the basic performance derived from the confusion matrix. Matrix confusion is a table that contains the results of binary calcification on test data. Algorithm testing is done using mathematical equations [27].

TP	FP
FN	TN

Figure 3. Confusion Matrix

Figure 3 shows the data obtained based on the confusion matrix system testing. There are True Positive (TP), True Negative (TN), False positive (FP), and False Negative (FN) values. By using the confusion matrix, the precession, recall, F1-score, and accuracy can be calculated.

Accuracy is the number of correct predictions made compared to the total number of predictions made, calculated by using the accuracy Equation 1 as follows:

$$\text{Accuracy} = \frac{TP}{TP + FN} \quad (1)$$

Precision is to calculate the number of cases predicted as positive by the model that should be predicted as positive, calculated by using the precession Equation 2 as follows:

$$\text{Precision} = \frac{TP}{TP + FP} \quad (2)$$

Recall is to calculate how well the model has classified positive examples, calculated by using the recall Equation 3 as follows:

$$\text{Recall} = \frac{TP}{TP + FN} \quad (3)$$

F1_score is the weighted harmonic average of precession and recall, and the Equation 4 is as follows:

$$F1 - score = \frac{2(\text{Precision} \times \text{Recall})}{\text{Precision} + \text{Recall}} \quad (4)$$

3. Results and Discussion

This section explains the results of research and at the same time provides comprehensive discussion. Results were presented in figures, graphs, tables and others that make the readers understand easily [28]. The discussion was divided in several sub-sections.

3.1 Dataset

The pneumonia dataset used retrieved from the Kaggle data repository. The dataset contained x-ray images of patients with pneumonia and normal patients, in jpeg format, with various dimensions including 1857 x 1317, 2031 x 1827 and many other sizes, with a total of 5,856 data. Data were selected from a retrospective cohort of pediatric

patients aged one to five years from Guangzhou Women and Children's Medical Center, Guangzhou. The image color model was grayscale with 8 bit deep color. All chest X-ray imaging was performed as part of the patients' routine clinical care. This study used 5856 image data.



Figure 4. Rotgen Image of the Thorax

Figure 4 is a thoracic rotgen figure, which is a type of medical examination that uses X-rays to produce internal figures of the organs of the chest. In a thoracic rotgen figure, these organs will be seen as gray shadows on a black background, allowing doctors to evaluate medical conditions and problems such as pneumonia. This dataset were used in the research and were carried out in the preprocessing and segmentation stages.

3.2 Preprocessing

Preprocessing is the initial stage in the analysis of rotgen thorax images. In the preprocessing stage, the rontgen thorax images obtained from the kaggle.com website were processed by resizing and converting the images.

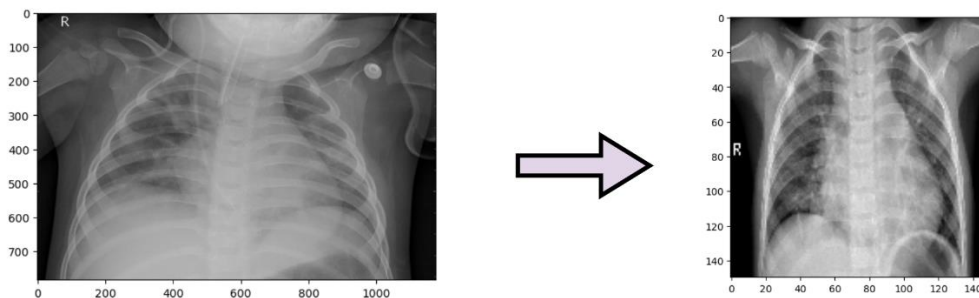


Figure 5. Resizing Result

Figure 5 is the result of resizing the initial stage of image processing to improve the quality and suitability of the image before continuing to the next stage of analysis. Resizing aimed to remove irrelevant noise parts in the image by removing pixels outside the important area. Resizing needs to be done to equalize the image size to facilitate classification in further research. The previous size of 800 x 1196 becomes 150x150 after resizing.

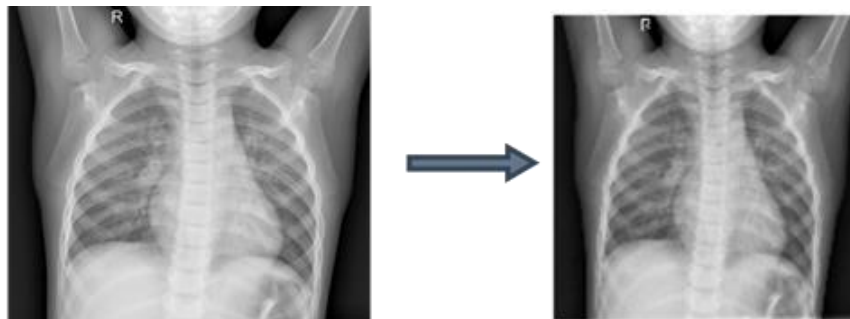


Figure 6. Image Conversion Result

Figure 6 is the result of image conversion where the initial image before image conversion is grayscale, image conversion is still done because of the efficiency of storage. The converted image has a smaller size than the unconverted grayscale image. Image conversion can improve the performance of machine learning algorithms.

3.3 Segmentation

Data that has been preprocessed were segmented. This segmentation used 4 thresholds in segmentation, namely thresh binary, thresh binary inv, thresh tozero and thresh tozero inv. The threshold value used is 150. The image results of the threshold can be seen in Figure 7.

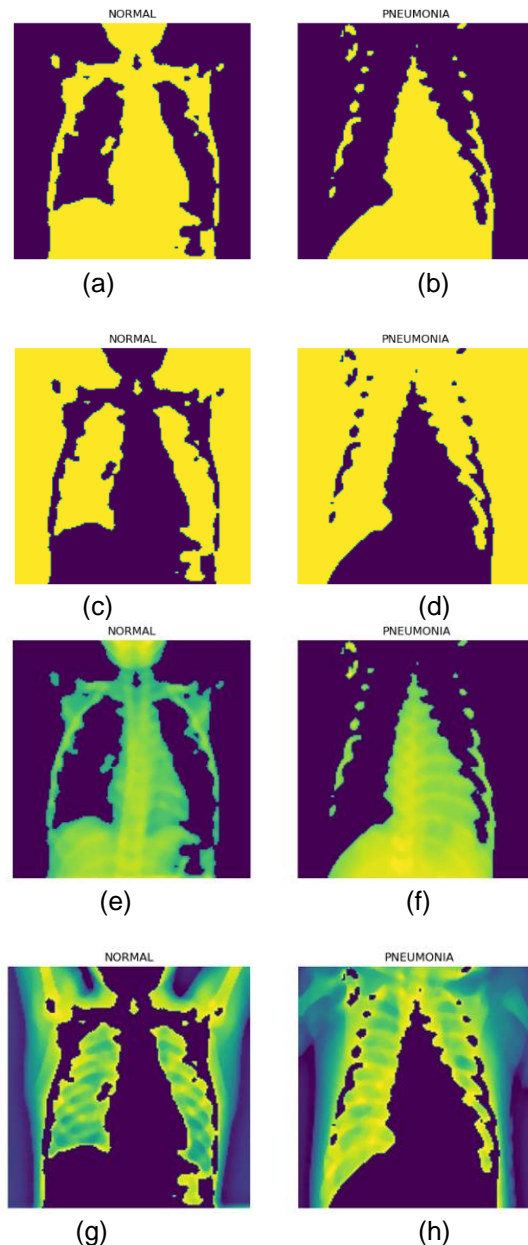


Figure 7. (a)(b)(c)(d)(e)(f)(g)(h) Output image threshold 150

Figure 7 (a) (b) are the results of the thresh_binary image. Figure 7 (a) is the results of pneumonia image data in the normal class where binary 0 is more dominant than binary 1. The results of pneumonia image data in the pneumonia class in Figure 7 (b) has the same result which is more dominant binary 0 than binary 1. Figure 7 (c) (d) are the results of thresh_binary_INV. Figure 7 (c) is the result of pneumonia image data in normal class where binary 1 is more dominant than binary 0, and the result of pneumonia image data in pneumonia class in Figure 7 (d) has the same result which is more dominant binary 1 than binary 0.

Figure 7 (e) (f) are the results of thresh_tozero. Figure 7 (e) is the result of pneumonia image data in the normal class where binary 0 is more dominant than binary 1, and the results of pneumonia image data in the pneumonia class in Figure 7 (f) has the same result which is more dominant binary 0 than binary 1. Figure 7 (g) (h) are the results of thresh_tozero_INV. Figure 7 (g) shows that the normal class pneumonia image data where binary 1 is more dominant

than binary 0, and the pneumonia class pneumonia image data in Figure 7 (h) has the same result which is more dominant binary 1 than binary 0.

3.4 Training model

This training used adam optimization which helped the model in training. Adam optimization is one of the methods used to calculate the learning rate for each different parameter. The dataset used in this study was 5,856 rontgen thorax data. With such a large amount of data, it took a long time to train the data simultaneously because the memory in the computer had limitations and required parameters, such as batch size and epoch. Batch size is a parameter that divides the dataset into several groups. The model training process was carried out by using Epoch 10. The training results in this study can be seen in Table 1.

Table 1. Training Result of Epoch Process

Epoch	Thresh_binary		Thresh_binary_inv		Thresh_tozero		Thresh_tozero_inv	
	Loss	Accuracy	Loss	Accuracy	Loss	Accuracy	Loss	Accuracy
1	1,3387	0,8263	1,4977	0,8149	1,7428	0,8008	1,2456	0,8005
2	0,4345	0,8697	0,2927	0,8975	0,6561	0,8710	0,3385	0,8716
3	0,3212	0,9030	0,2034	0,9233	0,3123	0,9047	0,2014	0,9182
4	0,2024	0,9030	0,2245	0,9233	0,1939	0,9319	0,1503	0,9405
5	0,1367	0,9275	0,2627	0,9239	0,1372	0,9483	0,1200	0,9511
6	0,1150	0,9532	0,1490	0,9507	0,1315	0,9540	0,1112	0,9511
7	0,1121	0,9532	0,1088	0,9576	0,1009	0,9639	0,1054	0,956
8	0,1174	0,9595	0,0942	0,9646	0,1009	0,9639	0,0768	0,9726
9	0,0951	0,9650	0,0790	0,9734	0,0885	0,9673	0,0641	0,9749
10	0,0699	0,9762	0,0785	0,9726	0,0806	0,9692	0,0536	0,9793

Table 1 represents the training results over several periods for different threshold techniques. For the highest loss value, with a value of 1.2456 at thresh_tozero it shows that the model predictions deviated significantly from the actual values in this period. The lowest loss value of 0.0536 at thres_tozero_inv shows that the model prediction is very much in line with the actual value. Thus indicating a well-trained model with an effective threshold. The highest accuracy value thres_tozero_inv shows an accuracy of 0.9793, this shows that at the 10th epoch the model trained with this threshold approach shows superior prediction. The lowest accuracy thresh_tozero shows an accuracy of 0.8005, this shows that at the beginning the model is lower than the other models. The epoch process results displayed from the training loss and training accuracy function values help evaluate the effectiveness of the model in classifying the train data, as well as improve each epoch process during training.

The results of Table 1 in graphical form can be seen in Figure 8 accuracy and loss graph of thres_binary, Figure 9 accuracy and loss graph of thres_binary_inv, Figure 10 accuracy and loss graph of thres_tozero, and Figure 11 accuracy and loss graph of thres_tozero_inv.

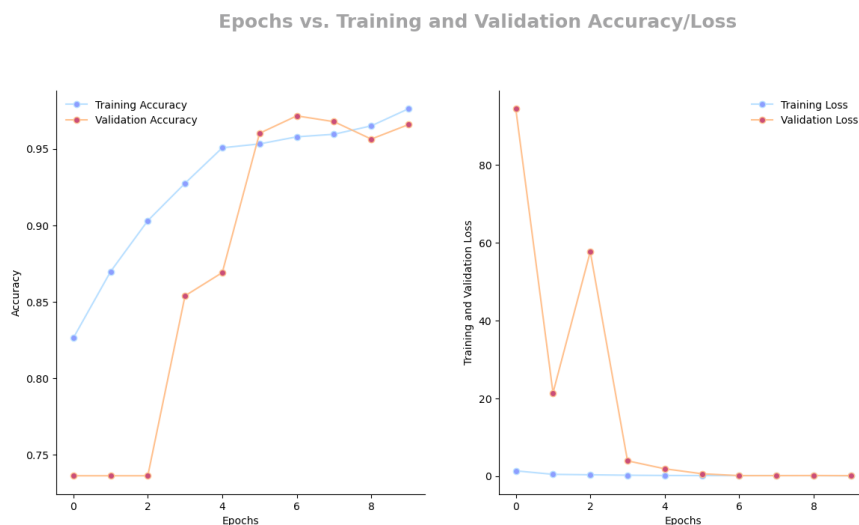


Figure 8. Accuracy and Loss Graph of thres_binary

Epochs vs. Training and Validation Accuracy/Loss

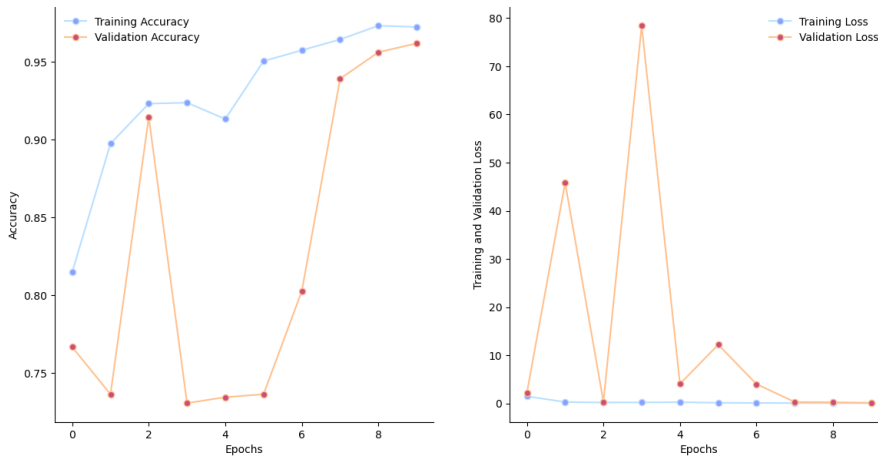


Figure 9. Accuracy and Loss Graph of thres_binary_inv
Epochs vs. Training and Validation Accuracy/Loss

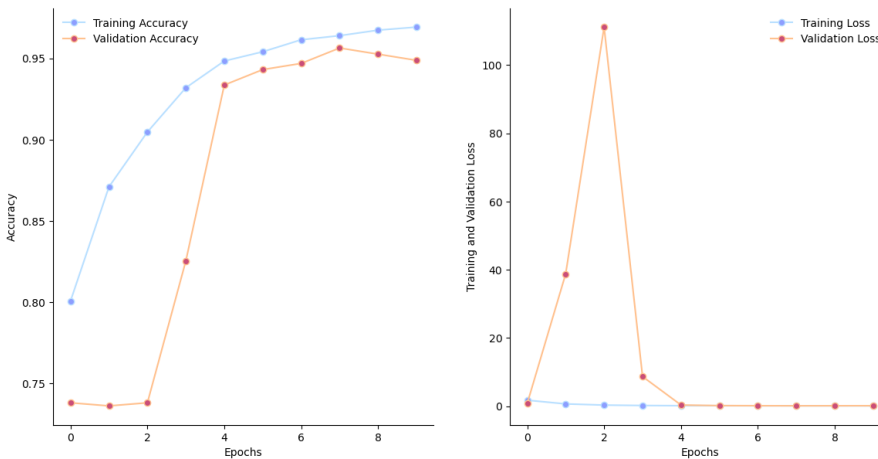


Figure 10. Accuracy and Loss Graph of thres_tozero

Epochs vs. Training and Validation Accuracy/Loss

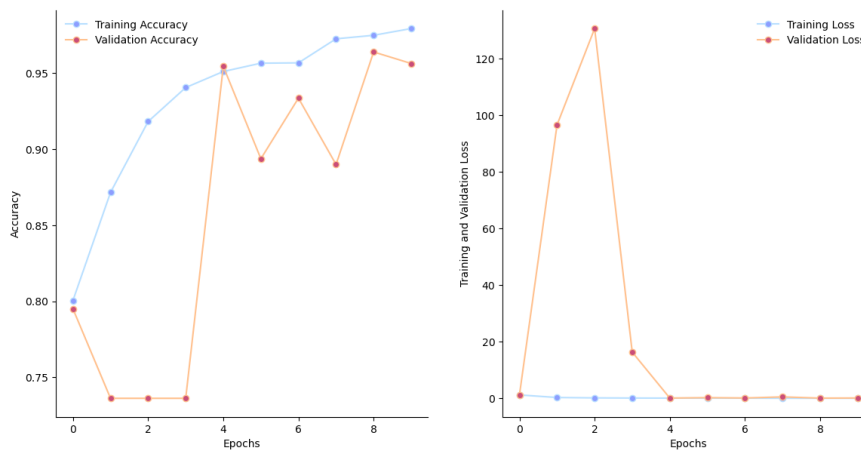


Figure 11. Accuracy and Loss Graph of thres_tozero_inv

Figure 8, Figure 9, Figure 10, and Figure 11 show that the accuracy of the model increases with the number of epochs. At the beginning of the training, the accuracy of the model tended to be low, but over time the accuracy of the model increased significantly. This shows that the model is gradually practicing to classify the image better. At the same time, in the loss graph, it can be seen that the loss of the model decreased as the number of execution epochs increased. Loss is a measure of how far the model's prediction is from the true value, considering that the lower the loss value, the better the quality of the model's prediction. This study shows that the model succeeds in reducing the loss significantly over time.

Table 2. Classification Results

class	Thresh_binary		Thresh_binary_inv		Thresh_tozero		Thresh_tozero_inv	
	true	false	true	false	true	false	true	false
Normal	135	27	144	18	152	10	152	10
Pneumonia	420	4	408	16	406	18	399	25
Accuracy%	95%		94%		95%		94%	

Table 2 is a table of classification results from testing models with CNN architecture. From the accuracy results, it shows that the segmentation technique has high accuracy both `thres_binary`, `thres_binary_inv`, `thres_tozero`, `thres_tozero_inv`. The highest accuracy value of 95% is obtained by `thres_binary` and `thres_tozero`, while 94% accuracy is obtained by `thres_binary_inv` and `thres_tozero_inv`. This shows that the segmentation technique in the CNN algorithm has high accuracy.

4. Conclusion

This research was conducted to identify rontghen thorax medical images by using 4 variants of segmentation techniques with the threshold value of 150. The purpose of this research is to produce a more accurate accuracy value and find out which segmentation technique produces the highest accuracy value. This research shows that the highest accuracy value is 95% with the segmentation techniques used are `thres_binary` and `Thres to_zero`. Meanwhile, `thres_binary_inv` and `Thres to_zero_inv` get an accuracy value of 94%. This shows that models that use segmentation techniques can classify images very well.

References

- [1] T. Gabruseva, D. Poplavskiy, dan A. Kalinin, "Deep learning for automatic pneumonia detection," *IEEE Comput. Soc. Conf. Comput. Vis. Pattern Recognit. Work.*, vol. 2020-June, hal. 1436–1443, 2020. <https://doi.org/10.1109/CVPRW50498.2020.00183>
- [2] A. U. Ibrahim, M. Ozsoz, S. Serte, F. Al-Turjman, dan P. S. Yakoi, "Pneumonia Classification Using Deep Learning from Chest X-ray Images During COVID-19," *Cognit. Comput.*, no. 0123456789, 2021. <https://doi.org/10.1007/s12559-020-09787-5>
- [3] N. Chebib dkk., "Pneumonia prevention in the elderly patients: the other sides," *Aging Clin. Exp. Res.*, vol. 33, no. 4, hal. 1091–1100, 2021. <https://doi.org/10.1007/s40520-019-01437-7>
- [4] D. Varshni, K. Thakral, L. Agarwal, R. Nijhawan, dan A. Mittal, "Pneumonia Detection Using CNN based Feature Extraction," *Proc. 2019 3rd IEEE Int. Conf. Electr. Comput. Commun. Technol. ICECCT 2019*, hal. 1–7, 2019. <https://doi.org/10.1109/ICECCT.2019.8869364>
- [5] Q. Wang, D. Yang, Z. Li, X. Zhang, dan C. Liu, "Deep regression via multi-channel multi-modal learning for pneumonia screening," *IEEE Access*, vol. 8, hal. 78530–78541, 2020. <https://doi.org/10.1109/ACCESS.2020.2990423>
- [6] E. Ayan dan H. Murat, "Diagnosis of Pneumonia from Chest X-Ray Images using Deep Learning," hal. 0–4, 2019.
- [7] H. Ren dkk., "Interpretable Pneumonia Detection by Combining Deep Learning and Explainable Models with Multisource Data," *IEEE Access*, vol. 9, hal. 95872–95883, 2021. <https://doi.org/10.1109/ACCESS.2021.3090215>
- [8] I. Bakti, M. Firdaus, T. Informasi, dan T. Industri, "Klasifikasi File Gambar Hasil X-Ray Paru-Paru Dengan Arsitektur Convolution Neural Network (CNN)," *J. Inf. Technol.*, vol. 3, no. 1, hal. 26–34, 2023.
- [9] L. Hernando dan A. Avaldo, "Implementasi Fuzzy Logic pada Alat Pemisah Buah Tomat," *J. Sains dan Inform.*, vol. 4, no. 1, hal. 55–61, 2022. <https://doi.org/10.22216/jsi.v8i2.1637>
- [10] R. Shinta, Jasril, M. Irsyad, F. Yanto, dan S. Sanjaya, "Klasifikasi Citra Penyakit Daun Tanaman Padi Menggunakan CNN dengan Arsitektur VGG-19 Rahma," *J. Sains dan Inform.*, vol. 4, no. 1, hal. 37–45, 2018. <https://doi.org/10.22216/jsi.v9i1.2175>
- [11] J. Yopento, E. Ernawati, dan F. F. Coastera, "Identifikasi Pneumonia Pada Citra X-Ray Paru-Paru Menggunakan Metode Convolutional Neural Network (CNN) Berdasarkan Ekstraksi Fitur Sobel," *Rekursif J. Inform.*, vol. 10, no. 1, hal. 40–47, 2022. <https://doi.org/10.33369/rekursif.v10i1.17247>
- [12] Z. Luo, W. Yang, Y. Yuan, R. Gou, dan X. Li, "Semantic segmentation of agricultural images: A survey," *Inf. Process. Agric.*, no. xxxx, hal. 1–15, 2023. <https://doi.org/10.1016/j.inpa.2023.02.001>
- [13] J. M. Adam dkk., "Deep learning-based semantic segmentation of urban-scale 3D meshes in remote sensing: A survey," *Int. J. Appl. Earth Obs. Geoinf.*, vol. 121, no. June, hal. 103365, 2023. <https://doi.org/10.1016/j.jag.2023.103365>
- [14] M. Hasan Jahid, M. Alom Shahin, dan M. Ali Shikhar, "Deep Learning based Detection and Segmentation of COVID-19 Pneumonia on Chest X-ray Image," *2021 Int. Conf. Inf. Commun. Technol. Sustain. Dev. ICICT4SD 2021 - Proc.*, hal. 210–214, 2021. <https://doi.org/10.1109/ICICT4SD50815.2021.9396878>
- [15] R. Zhang, G. Li, T. Wunderlich, dan L. Wang, "A survey on deep learning-based precise boundary recovery of semantic segmentation for images and point clouds," *Int. J. Appl. Earth Obs. Geoinf.*, vol. 102, hal. 102411, 2021. <https://doi.org/10.1016/j.jag.2021.102411>
- [16] S. Wang, D. M. Yang, R. Rong, X. Zhan, dan G. Xiao, "Pathology Image Analysis Using Segmentation Deep Learning Algorithms," *Am. J. Pathol.*, vol. 189, no. 9, hal. 1686–1698, 2019. <https://doi.org/10.1016/j.ajpath.2019.05.007>
- [17] R. F. Nugrohputri dkk., "Segmentasi Citra Nukleus Sel Kanker Serviks Menggunakan Otsu Thresholding dan Morfologi Closing," *JSI J. ...*, vol. 14, no. 1, hal. 2533–2543, 2022.

- [18] A. Yudhana, R. Umar, dan S. Saputra, "Fish Freshness Identification Using Machine Learning: Performance Comparison of k-NN and Naïve Bayes Classifier," *J. Comput. Sci. Eng.*, vol. 16, no. 3, hal. 153–164, 2022. <https://doi.org/10.5626/JCSE.2022.16.3.153>
- [19] R. T. Wahyuningrum *dkk.*, "Segmentasi Citra X-Ray Dada Menggunakan Metode Modifikasi Deeplabv3+," vol. 10, no. 3, hal. 687–698, 2023. <https://doi.org/10.25126/jtiik.20231036754>
- [20] S. Saputra, A. Yudhana, dan R. Umar, "Implementation of Naïve Bayes for Fish Freshness Identification Based on Image Processing," *J. RESTI (Rekayasa Sist. dan Teknol. Informasi)*, vol. 6, no. 3, hal. 412–420, 2022. <https://doi.org/10.29207/resti.v6i3.4062>
- [21] M. Furqan, A. Aulia, dan Sriani, "Algoritma K-Means Untuk Segmentasi Kematangan Buah Jeruk Berdasarkan Kemiripan Warna," *J. Sains Komput. Inform.*, vol. 6, no. 1, hal. 199–208, 2022.
- [22] I. K. Adi Bayu Adnyana, I. M. Oka Widyantara, dan N. Dewi Wirastuti, "Analisa Metode Shannon Entropy Dan Differential Evolution Untuk Kompresi Gambar," *J. SPEKTRUM*, vol. 8, no. 2, hal. 221, 2021. <https://doi.org/10.24843/SPEKTRUM.2021.v08.i02.p25>
- [23] A. Yudhana, Sunardi, dan S. Saifullah, "Segmentation comparing eggs watermarking image and original image," *Bull. Electr. Eng. Informatics*, vol. 6, no. 1, hal. 47–53, 2017. <https://doi.org/10.11591/eei.v6i1.595>
- [24] P. K. Sahoo, S. Soltani, dan A. K. C. Wong, "A survey of thresholding techniques," *Comput. Vision, Graph. Image Process.*, vol. 41, no. 2, hal. 233–260, 1988. [https://doi.org/10.1016/0734-189X\(88\)90022-9](https://doi.org/10.1016/0734-189X(88)90022-9)
- [25] N. Nafi'iyah dan E. Setyati, "Lung X-Ray Image Enhancement to Identify Pneumonia with CNN," *East Indones. Conf. Comput. Inf. Technol.*, hal. 421–426, 2021.
- [26] A. Fadlil dan D. Prayogi, "Sistem Pengenalan Wajah pada Keamanan Ruang Berbasis Convolutional Neural Network," vol. 6, no. September, hal. 636–647, 2022.
- [27] N. Abdillah, A. K. W. Hapantenda, A. Habib, dan I. Listiowarni, "Klasifikasi Viral Pneumonia Menggunakan Metode Convolutional Neural Network Dan Support Vector Machine," *Konvergensi*, vol. 18, no. 2, hal. 50–56, 2022. <https://doi.org/10.30996/konv.v18i1.6916>
- [28] B. Boehm, *Barry Boehm Software Engineering Economics*, vol. 10, no. 1. Prentice-hall, 1984.

